Environmental Research Letters

LETTER

Three centuries of dual pressure from land use and climate change on the biosphere

Sebastian Ostberg[1], **Sibyll Schaphoff**[1], **Wolfgang Lucht**[1,2] **and Dieter Gerten**[1]

[1] Research Domain 1 Earth System Analysis, Potsdam Institute for Climate Impact Research, Telegraphenberg A62, D-14473 Potsdam, Germany

[2] Department of Geography, Humboldt-Universität zu Berlin, Berlin, Germany

E-mail: sebastian.ostberg@pik-potsdam.de

Keywords: land use change, climate change, impacts, biogeochemistry, biosphere

Supplementary material for this article is available online

OPEN ACCESS

RECEIVED
5 December 2014

REVISED
18 March 2015

ACCEPTED FOR PUBLICATION
26 March 2015

PUBLISHED
15 April 2015

Abstract

Human land use and anthropogenic climate change (CC) are placing mounting pressure on natural ecosystems worldwide, with impacts on biodiversity, water resources, nutrient and carbon cycles. Here, we present a quantitative macro-scale comparative analysis of the separate and joint dual impacts of land use and land cover change (LULCC) and CC on the terrestrial biosphere during the last ca. 300 years, based on simulations with a dynamic global vegetation model and an aggregated metric of simultaneous biogeochemical, hydrological and vegetation-structural shifts. We find that by the beginning of the 21st century LULCC and CC have jointly caused major shifts on more than 90% of all areas now cultivated, corresponding to 26% of the land area. CC has exposed another 26% of natural ecosystems to moderate or major shifts. Within three centuries, the impact of LULCC on landscapes has increased 13-fold. Within just one century, CC effects have caught up with LULCC effects.

1. Introduction

The Earth system is currently undergoing a large-scale transformation of many of its components, including the terrestrial biosphere, that has prompted the declaration of a new geological epoch: the Anthropocene (Steffen *et al* 2007). Natural ecosystems across the globe face mounting pressure from two anthropogenic processes, one direct, land use and land cover change (LULCC), and one indirect, climate change (CC). The transformation these two pressures cause is on-going, with wide-ranging implications from biodiversity, food security and human health to feedbacks with other components of the earth system. Two questions emerge: (1) What is the comparative strength of CC effects, which are a phenomenon largely of the recent decades, and LULCC effects, which have emerged in their current form over the course of the last 300 years mainly? (2) What is the combined magnitude of biosphere transformation caused by these pressures until today?

In light of the pervasiveness of present-day LULCC it has been suggested to characterize the land surface in terms of 'anthromes' instead of (natural) biomes (Ellis and Ramankutty 2008). Historical reconstructions trace back the spread of agriculture over several millennia (e.g. Kaplan *et al* 2011, Klein Goldewijk *et al* 2011), and the combination of satellite and census data helps to distinguish which crops are grown where (e.g. Portmann *et al* 2010). Biospheric impacts of CC have been documented on every continent and in most major taxonomic groups (Parmesan 2006) and were reviewed extensively, e.g., in IPCC (2014a chapters 4,18) and with regional focus in IPCC (2014b chapter 22–30).

We use multidimensional shifts in a number of basic biospheric properties as a proxy for more complex changes happening in ecosystems in response to LULCC and CC. The rationale behind this proxy approach is that significant changes of the fundamental building blocks, e.g. carbon and water exchanges with the atmosphere and soil, or broad types of vegetation in terms of their functional strategies, imply impacts on more detailed hierarchical structures, such as predator-prey and host-parasite relations (Parmesan 2006), complementarity and competition

Table 1. Parameters in the Γ metric describing landscape states.

Group	Individual parameters[a]
Carbon exchange fluxes	Net primary production, heterotrophic respiration *and harvest (from crops and grasslands)*, fire carbon emissions
Carbon stocks	Carbon contained in vegetation, sum of soils and litter
Water exchange fluxes	Transpiration, sum of soil evaporation and interception loss from vegetation canopies, runoff
Other system-internal processes	Fire frequency, soil water content *(upper 1 m, 3 layers)*
Vegetation structure	Composition of PFTs *and CFTs*

[a] Changes to original metric implementation marked in italics.

regarding resource use (Hooper *et al* 2005), or mutual interactions like pollination (Mooney *et al* 2009) that cannot be readily modelled at the global scale (Ostberg *et al* 2013).

Impacts of LULCC and CC on individual biospheric properties have been studied extensively, usually focussing on only one of the two pressures or modelling them at drastically diverging levels of complexity. For example, LULCC has reduced global transpiration by ≈10%, while increasing river discharge by 7%, as was found in a modelling study comparing present land use patterns to conditions of potential natural vegetation (PNV) (Rost *et al* 2008). The human appropriation of terrestrial net primary production has been estimated at 24% of total potential productivity (Haberl *et al* 2007), and has doubled over the course of the 20th century (Krausmann *et al* 2013). Emissions from LULCC have likely amounted to 156 Pg C (or 35% of all anthropogenic CO_2 emissions) between 1850 and 2000 (Houghton 2003, Pongratz *et al* 2008) and to 1.1 ± 0.7 Pg C yr^{-1} during the first decade of the 21st century, although their share of the total emissions has gone down considerably due to the increasing contribution from burning of fossil fuels (Friedlingstein *et al* 2010).

Observed CC impacts in terrestrial natural ecosystems include changes in phenology (e.g. spring advancement of ≈3 days per decade, Parmesan 2007), productivity and mortality as well as shifts in geographical ranges (on average 6 km per decade poleward, Parmesan and Yohe 2003), often combined with changes in species distributions and biodiversity. Based on modelling, CC and increased CO_2 concentrations have resulted in a long-term increasing trend in global river discharge of +26 km^3 yr^{-2} during the 20th century (Gerten *et al* 2008) and a cumulative land uptake of 70–110 Pg C during the second half of the 20th century (Sitch *et al* 2008). CO_2 fertilization alone has lead to an 11% increase of vegetation cover across warm, arid environments during recent decades (Donohue *et al* 2013).

Comparability between impact studies is often limited owing to a lack of a common baseline and lack of common or at least comparable indicators, and attribution of observed impacts is often difficult in the presence of multiple drivers of change (Stone *et al* 2013).

Here, we present an analysis of the impacts of LULCC and climate/CO_2 change for the last ≈300 years, based on a consistent framework composed of (1) observation-based global gridded climate data, (2) historical reconstructions of cropland and managed grassland areas, (3) a Dynamic Global Vegetation Model (DGVM) capable of simulating vegetation-soil dynamics of both natural vegetation and agricultural ecosystems, both at comparable levels of complexity, and (4) an aggregated metric of simultaneous biogeochemical, hydrological and structural shifts at the landscape (grid cell) scale.

We produce a time series of human intervention with the terrestrial biosphere from 1700 and present results for the joint and separate effects.

2. Materials and methods

Changes of the biosphere are quantified using the Γ metric of biogeochemical and vegetation-structural change (Heyder *et al* 2011). While Γ was originally designed to assess the risk of future CC to natural ecosystems, we extend it here to also analyse LULCC effects. The metric characterizes ecosystem states as vectors in a multidimensional state space where each dimension represents one exchange flux, pool or process variable (listed in table 1). The change between two states is then expressed as the length of the difference vector and the angle between state vectors (Heyder *et al* 2011). Γ is formulated to evaluate four equally weighted components of change:

$$\Gamma = \Big(\Delta V \cdot S\big(\Delta V, \sigma_{\Delta V}\big) + c \cdot S(c, \sigma_c) + g \cdot S(g, \sigma_g) + b \cdot S\big(b, \sigma_b\big)\Big)\Big/4, \quad (1)$$

where ΔV characterizes changes in vegetation structure, c is the local change component, g is the global importance component, b is the ecosystem balance component, and $S(x, \sigma_x)$ is a change to variability ratio.

Vegetation changes in terms of major ecological strategies (herbaceous versus woody, broadleaved versus needleleaved, evergreen versus deciduous) are expressed by ΔV, based on Sykes *et al* (1999), but with modifications to accommodate plant functional types (PFTs) in LPJmL (Ostberg *et al* 2013). For this study, we add a new attribute *naturalness* to distinguish

between natural and managed ecosystems (see online supporting information (SI) available at stacks.iop.org/erl/10/044011/mmedia).

Local change c quantifies biogeochemical changes relative to previously prevailing conditions at each location and therefore the magnitude of local landscape transformation. In contrast, g captures the contribution of local changes to global biogeochemistry, assuming that even moderate (relative) changes on the local scale may feed back to larger scales (global carbon cycle, atmospheric circulation patterns, downstream water availability). Ecosystem balance b is computed as the angle between state vectors and represents changes in the magnitude of biogeochemical properties relative to each other, which indicate alterations in the contributing dynamic processes and hence ecological functioning. S relates the change of each component $x \in (\Delta V, c, g, b)$ to its variability σ_x under reference conditions, reflecting the expectation that ecosystems are adapted to the range of year-to-year variability. All terms in (1) are scaled between 0 (no change) and 1 (very strong change) using sigmoid transformation functions as described in Heyder *et al* (2011).

Each grid cell in the model represents a landscape unit characterized by homogeneous forcing conditions (climate, soil, CO_2). Unless stated otherwise, LULCC and CC effects are assessed at grid cell level even though land use change has a direct effect only on the cropland or managed grassland portion of the cell. Parameters in table 1 are averaged across natural and managed parts before quantification of the total landscape state which is then used to derive landscape change.

Previous studies of CC impacts on natural vegetation used thresholds of $0.1 < \Gamma < 0.3$ and $\Gamma > 0.3$ to denote risk of moderate and major ecosystem transformation, respectively (Heyder *et al* 2011, Ostberg *et al* 2013, Warszawski *et al* 2013). For example, moderate changes in the Γ metric are comparable to the difference between similar, yet distinct biomes under present climate, such as temperate coniferous and temperate broadleaved forests, whereas a boreal evergreen forest differs from temperate forests by a Γ of 0.3–0.4 and a shift from a temperate forest to a savanna would result in Γ of ≈0.4–0.6 (see figure S2 in Ostberg *et al* 2013). None of these studies considered human land use. Quantified at the landscape scale, LULCC impacts scale with both the magnitude of change on the managed land and the fraction of the grid cell transformed.

2.1. Model description

The LPJmL DGVM simulates natural vegetation, represented by 9 PFTs (Sitch *et al* 2003), as well as agriculture, represented by 13 crop functional types (CFTs) and managed grasslands (Bondeau *et al* 2007). The current model version includes a permafrost module and a new hydrology scheme (Schaphoff *et al* 2013).

PFT composition within a grid cell is the result of competition between plant types for light, space and water. Establishment depends on climatic suitability and the density of the existing vegetation. Mortality rates depend on growth efficiency, plant density and climatic stress. For fire disturbance, daily fire probability is calculated based on fuel load and litter moisture, the annual burnt area fraction is derived from the length of the fire season, whereas the fraction of killed individuals within burnt areas depends on PFT-specific fire resistance (Thonicke *et al* 2001).

Crops and managed grasslands are grown on prescribed areas, and irrigation is possible on areas equipped for irrigation (section 2.2). Irrigation water demand is determined from the soil water deficit below optimal growth (Rost *et al* 2008). We assume that irrigation water withdrawal equals demand and is not limited by the local renewable water resource. Sowing dates for annual crops are computed within the model based on a set of rules depending on crop- and climate-specific characteristics (Waha *et al* 2012). Crops are harvested when they reach maturity, which is defined as a crop-specific phenological heat unit sum, at which point carbon from the storage organ pool is extracted. For annual crops, extensive grass growth is simulated outside the growing period as a proxy for inter-cropping practices. Managed grasslands are harvested whenever the above-ground carbon pool reaches a threshold, at which point 50% are extracted.

Plant growth of both natural vegetation and crops in LPJmL is constrained by temperature, radiation, water and CO_2 availability. Nutrients such as nitrogen and phosphorus are not explicitly modelled.

The model setup for this study assumes good management of crops everywhere instead of applying different management intensities per crop and country, which are not well-documented historically. Although management has an impact on Γ, we found its effect to be minor compared to the first-order effect of changing natural vegetation to cropland/managed grassland (see section S2 and figure S1 in the SI available at stacks.iop.org/erl/10/044011/mmedia).

The model runs on a spatial grid of 0.5° longitude by 0.5° latitude and a daily time step. It is driven by monthly temperature, precipitation, cloud cover and number of wet days (section 2.3) which are disaggregated according to Gerten *et al* (2004). Additional inputs include information on soil properties, country-specific irrigation efficiencies (Rohwer *et al* 2007), and annual atmospheric CO_2 concentrations (section 2.3).

Individual processes in LPJmL have been validated extensively before, e.g. Sitch *et al* (2003, 2008) for carbon cycling and plant geography of the natural vegetation, Bondeau *et al* (2007), Fader *et al* (2010) for crop production, Rost *et al* (2008) for irrigation water use

Table 2. Scenario setup. Each scenario is simulated with 20 different climate realizations as described in section 2.3.

Name	Description
PNV_{noCC}	Control scenario without any human impact, potential natural vegetation only, constant climate at 1901–1930 level and CO_2 at 282 ppm; reference run for full impact
PNV_{CC}	Scenario without land use (potential natural vegetation only), but with transient climate and CO_2; reference run for land use change effect
LUC_{noCC}	Scenario with transient land use, but with constant climate at 1901–1930 level and CO_2 at 282 ppm; reference run for climate change effect
LUC_{CC}	Representation of actual, transient land use, climate and CO_2; comparison with reference runs gives full impact, land use change effect, climate change effect

and Schaphoff *et al* (2013) for permafrost, river flow, carbon and water fluxes. LPJmL participates in model intercomparison projects, such as AgMIP (http://agmip.org), ISI-MIP (http://isi-mip.org), and the already finished WaterMIP (http://eu-watch.org/watermip).

2.2. Land use data

Annual fractions of 13 CFTs (12 distinct types and one mixed class of other annual and perennial crops) and managed grasslands in each 0.5° grid cell are prescribed with a distinction between irrigated and rainfed areas. Data for the year 2000 are taken from the MIRCA2000 dataset (Portmann *et al* 2010) and are extrapolated historically to the year 1700 based on the relative changes of cropland and pasture extent from the HYDE3 database (Klein Goldewijk and van Drecht 2006). The temporal evolution of irrigated areas is estimated from global trends (Hoekstra 1998). Compared to the documentation in Fader *et al* (2010) the current dataset version has been extended to include sugarcane as a separate CFT. Areas not covered by managed lands are assumed to be covered with natural vegetation or barren, as dynamically simulated by LPJmL.

In the context of this study, LULCC refers to the conversion and use of land as cropland or managed grassland. Other forms of land use such as forest management are not considered.

2.3. Climate data

We use observation-based monthly temperature and cloud cover time series provided by the Climatic Research Unit (CRU TS version 3.21) and spanning 1901–2012 (CRU *et al* 2013, Harris *et al* 2014). These are combined with gridded precipitation provided by the Global Precipitation Climatology Centre (GPCC Full Data Reanalysis Version 6.0), spanning 1901–2010 (Schneider *et al* 2011, Becker *et al* 2013), which is extended to cover the full CRU land mask. The corresponding number of wet days per month, used to distribute monthly precipitation sums, is derived synthetically using the CRU approach (New *et al* 2000, Heinke *et al* 2013).

We use early 20th century (1901–1930) observations before 1900. Since detection and attribution studies have identified human activities as the dominant driver of observed climate changes during the second half of the 20th century (IPCC 2013), early 20th century is a suitable reference to calculate climate-driven changes. For this, the first 30 years of observation-based data are randomly reshuffled into a new sequence spanning 1700–1900. Since reshuffling may change some properties of the original statistical distribution, we produce 20 different realizations and run simulations for all of them. Atmospheric CO_2 concentrations are based on merged ice-core record data for 1830–1958, provided by Scripps Institution of Oceanography (http://scrippsco2.ucsd.edu/data/atmospheric_co2.html, Keeling *et al* 2001), and on direct observations from the Mauna Loa Observatory after 1958, provided by NOAA/ESRL (http://esrl.noaa.gov/gmd/ccgg/trends/, both datasets as of 31 March 2014). A constant concentration of 282 ppm is used before 1830. No distinction between anthropogenic and natural contributions to CC is made in the analysis of impacts.

2.4. Simulation setup

LPJmL simulations require a spin up of 5000 years for vegetation and soil carbon pools to reach an equilibrium state. Spin up is performed for PNV without any land use, but with fire disturbance and dynamic vegetation, recycling the 200-year climate sequence and constant CO_2 concentration described above. We run four scenarios from 1700–2010, as described in table 2. The LUC scenarios are preceded by another 100 years of spin up using the land use pattern from 1700 to adjust carbon stocks from the PNV spin up and train sowing dates, which are based on climate experienced in the past. All four scenarios are simulated for each of the 20 climate realizations. LUC_{CC} and PNV_{CC} runs use transient atmospheric CO_2 from 1830 and transient CRU/GPCC climate data from 1901. In contrast, LUC_{noCC} and PNV_{noCC} runs use a constant CO_2 concentration of 282 ppm and continue using the reshuffled constant climate sequence after 1900. The difference between the various simulations allows us to separate the individual effects of LULCC and CC (see table 2).

Landscape states for the Γ metric are compared using 30 year averages of the state variables to avoid

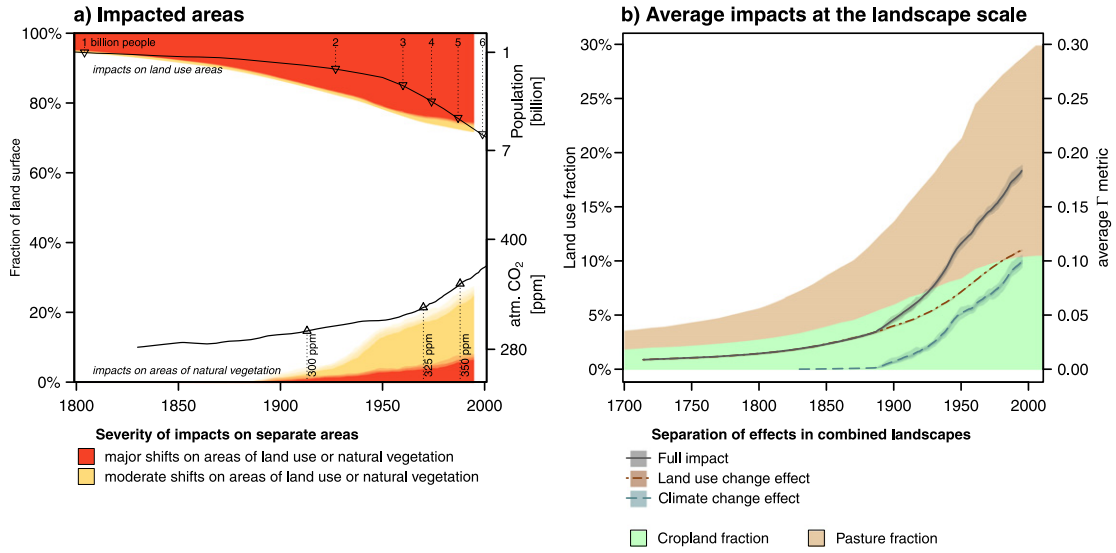

Figure 1. Transformation of natural ecosystems through land use and climate change. (a) Impacts on land use areas shown from above, impacts on remaining natural ecosystems shown from below. Remaining white area represents natural vegetation with only minor climate change impacts. World population and atmospheric CO_2 concentration added for illustrative purposes. (b) Average impacts (full, LULCC, CC) quantified at the landscape scale. Lines and coloured shading depict ensemble mean and ensemble range, respectively. Background shading shows land use fraction.

noise from inter-annual variability. We derive the full impact of human land use and CC (we include increasing CO_2 in the latter) on landscapes by comparing the LUC_{CC} (real world) scenario to the PNV_{noCC} control scenario. The difference between LUC_{CC} and LUC_{noCC} gives the CC effect, while a comparison between LUC_{CC} and PNV_{CC} provides an estimate of the land use change effect (table 2). Time series of these effects are derived from concurrent time frames of the respective scenarios. Global and biome aggregates are calculated as area-weighted means of the grid cell values.

Γ values for the separated effects do not necessarily add up to the full impact value. This is due to possibly opposing impacts of climate and LULCC. Only the full impact is based on constant reference conditions (PNV_{noCC}, table 2), whereas reference conditions for the CC effect (LUC_{noCC}) and land use change effect (PNV_{CC}) are themselves impacted by land use and CC, respectively.

3. Results and discussion

3.1. Global development

By the beginning of the 21st century, humans have transformed almost 30% of the global ice-free land area for agricultural production, replacing the original natural ecosystems. Quantifying Γ separately on the cultivated areas, more than 90% of croplands and pastures, corresponding to 26% of the global land area, have experienced major biogeochemical and structural shifts ($\Gamma > 0.3$), with moderate changes ($0.1 < \Gamma < 0.3$) on the rest (figure 1(a)). These changes were driven mainly by LULCC, but also include CC impacts on cultivated lands. Natural ecosystems covering an additional 26% of the land surface have experienced major or at least moderate climate-driven changes (figure 1(a)).

The majority of landscapes contain a mixture of natural and agricultural ecosystems. Within landscapes, effects of land use may be partially offset by CC and vice versa. For example, forest clearing reduces carbon stocks on the cultivated fraction, but enhanced productivity through warming or CO_2 fertilization may increase carbon stocks in the remaining natural vegetation. The full impact within these landscapes is therefore the combined effect of LULCC and CC. As a global average, LULCC and CC together have transformed landscapes worldwide by a value of $\Gamma = 0.18$ (full impact, figure 1(b)). This includes major impacts in 24% in addition to moderate changes in 31% of all landscapes (table 3, figure 2(b)).

Our simulation setup allows us to separate the LULCC effect from the CC effect within landscapes/grid cells where they co-occur. During the time frame of our analysis, total agricultural area has expanded from roughly 500 Mha to almost 4300 Mha. Compared to the PNV_{CC} world, land use change has caused an average impact on landscapes of $\Gamma = 0.009$ during 1700–1729 and $\Gamma = 0.11$ today in the LUC_{CC} simulations (figure 1(b)).

In parallel, atmospheric CO_2 concentration has risen from 282 ppm in 1830 to 390 ppm in 2010, and long-term annual mean temperature on land (computed as an area-weighted 30-year mean across all simulated grid cells) has risen by almost 0.8 K within 80 years. This has resulted in an average change of $\Gamma = 0.1$ today (figure 1(b)).

Table 3. Global impacts and affected areas quantified at the landscape scale. Values provided for two 30-year time slices centred on 1915 and 1995, as in figure 2.

Impact	1901–1930	1981–2010
Full impact		
Global average Γ	0.06	0.18
Fraction of land area with:		
$0.1 < \Gamma < 0.3$	12%	31%
$\Gamma > 0.3$	6%	24%
Land use change effect		
Global average Γ	0.05	0.11
Fraction of land area with:		
$0.1 < \Gamma < 0.3$	10%	16%
$\Gamma > 0.3$	5%	15%
LUC effect dominant	44%	40%
Climate change effect		
Global average Γ	0.01	0.1
Fraction of land area with:		
$0.1 < \Gamma < 0.3$	2%	23%
$\Gamma > 0.3$	2%	10%
CC effect dominant	56%	60%
of which free of agriculture	62%	53%

Hence, LULCC and CC have reached the same level, although marked differences underlie the global aggregate impact.

CC is currently the dominating effect on 60% of the land surface (table 3, figure 2(f)). Half of this area is virtually agriculture-free (<1% of grid-cell area used), while the other half contains on average 27% managed lands. In the remaining 40% of landscapes (of which on average 52% are used as cropland or pasture), the LULCC effect exceeds the CC effect (table 3, figure 2(d)). At the beginning of the 20th century (1901–1930), the share between landscapes with dominant climate or land use change effects was similar (56% and 44% of the land surface, table 3), but average impacts were one order of magnitude smaller for climate and less than half for land use.

It is worth noting that in the vast majority of landscapes the dominant effect is at least 5 times as strong as the secondary effect. There are very few landscapes where climate and land use effects are of similar magnitude. Examples include some boreal and tropical forests with minor CC impacts and low fractions of land use, or some Chinese steppe regions with mostly moderate CC and moderate to major LULCC impacts (figures 2(b), (d) and (f)).

3.2. Historical evolution of LULCC impacts

Although humanity has practiced agriculture at least since the early Holocene (Kirch 2005), almost 90% of the current cropland and managed grassland extent have been converted within the last 300 years. In 1700, almost 60% of all landscapes were still virtually free of agriculture (<1% of their area transformed), and in most other landscapes land use density was low (98% of all landscapes with <25% use, figure S2 in the SI). Regions with higher land use density were limited to Western and Central Europe and parts of China. Major change at the landscape scale (land use change effect, $\Gamma > 0.3$) was limited to <1% of the land surface, mostly in Ireland and France, but also along the Nile river in Egypt and in some parts of Pakistan, while land use caused only minor changes ($\Gamma < 0.1$) in the majority of landscapes.

By 1800, areas with major land use impacts had expanded to Northern India and parts of Western China, but still encompassed only 1.2% of the land surface. Although half of all landscapes were already partly cultivated, land use density was low in most of them, causing only minor impacts.

Land use expansion accelerated during the 19th century, and by 1900 5% of all landscapes were dominated by land use (>50% of their area transformed), while a quarter of all landscapes contained at least 25% land use. This caused at least moderate changes ($\Gamma > 0.1$) in 13% of all landscapes. Agriculture had also expanded into new regions, especially North America, with now only about one third of global landscapes left agriculture-free. However, croplands and managed grasslands had still only achieved roughly half of their present-day global extent.

During the 20th century, agricultural expansion mainly took place in landscapes that already contained some portion of land use. The share of landscapes with more than 25% croplands and pastures doubled, and the share of landscapes with more than 50% use increased six-fold. This is reflected in the here studied LULCC effect: while the global average Γ increased from 0.04 to 0.11, the fraction of landscapes with major change ($\Gamma > 0.3$) almost quadrupled from 4 to 15%. Today, only one third of all landscapes can still be considered free of agriculture (<1% of their area transformed), while almost as many landscapes are now dominated by managed lands (>50% of their area transformed, figure S2 in the SI).

As with any historical reconstruction, a caveat of the HYDE database used here is that it has considerable uncertainties based on input data (primarily population data) and assumptions and parameters (primarily change in land use per capita over time) used in its construction (Ellis *et al* 2013, Klein Goldewijk and Verburg 2013). For example, based on a scenario of adaptive changes in land use systems, the KK10 model (Kaplan *et al* 2011) produces consistently higher levels of pre-industrial land cover change, and roughly twice as much land use change in 1850 as HYDE. However, both reconstructions converge towards the present. Naturally, the uncertainty of historical LULCC patterns translates into the evolution of the here studied LULCC effect. Given their convergence, our results for the second half of the 20th century and the comparison with recent CC impacts should remain relatively unaffected by the choice of land use reconstruction.

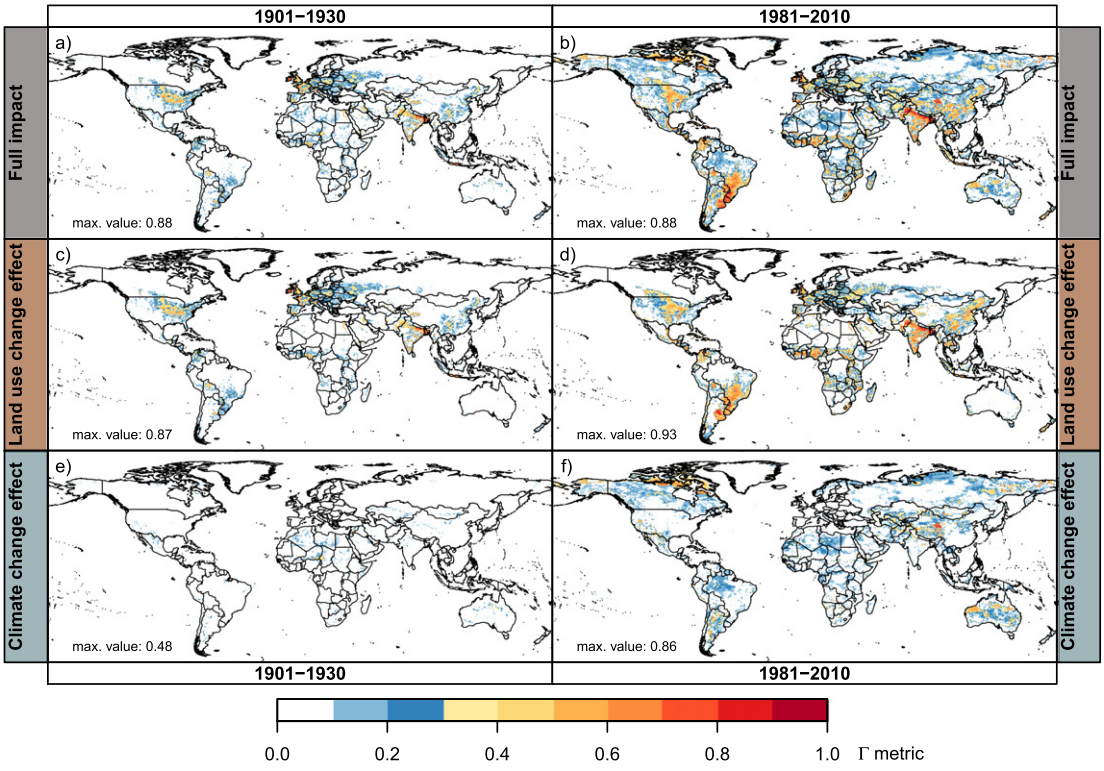

Figure 2. Spatial patterns of impacts on the biosphere. Full impact (a), (b), land use change effect (c), (d) and climate change effect (e), (f) shown for two 30-year time slices centred on 1915 and 1995 (left and right, respectively). All effects quantified at the landscape (i.e. grid cell) scale. Maps depict ensemble mean from 20 climate realizations.

3.3. Biome-level changes

At present, temperate broadleaved deciduous and evergreen forests show the highest full impact with values of $\Gamma = 0.39$ and $\Gamma = 0.30$, respectively (figure 3). Land use change is the main driver of Γ in temperate forests, where the average LULCC effect is roughly 4–9 times higher than the CC effect. The impact of land use decreases from temperate forests to savannas to grasslands, the latter having a land use change effect of only $\Gamma = 0.07$ despite 54% of their area being used predominantly as managed grasslands. On the other hand, there is a sharp increase of the CC effect along this gradient, with forests experiencing an average Γ of 0.04–0.05 compared to $\Gamma = 0.13$ in grasslands.

In the tropics, the average CC effect is almost equal between tropical rainforests and warm grasslands ($\Gamma = 0.09$), with slightly lower impacts in warm woody savannas and tropical seasonal forests and considerably higher impacts ($\Gamma = 0.14$) in open savannas. In terms of the LULCC effect, there is a similar increasing trend from warm grasslands to savannas to tropical seasonal forests as in the temperate zone. Tropical rainforests have less than half as much land use share as the other tropical biomes, resulting in a lower land use $\Gamma = 0.12$ (figure 3).

Averaged across the whole biome, LULCC and CC effects are at an equal level in boreal forests. Climate impacts are higher than in other forests (except tropical rainforests), but land use effects are low given that only 14–16% of their potential natural extent have been converted to croplands and pastures. Overall, boreal forests have the lowest average full impact of all biomes with $\Gamma = 0.12$. While tundra regions have the lowest land use share with only 6% of their pre-industrial extent, they have been exposed to the strongest CC impacts, with an average CC effect of $\Gamma = 0.2$ (figure 3).

Figure S3 and section S3 in the SI (available at stacks.iop.org/erl/10/044011/mmedia) illustrate the different ways in which LULCC and CC affect the components that constitute Γ in each biome.

Comparing the temperate and tropical zone illustrates that the land use change effect depends not only on the fraction of the landscape that is transformed, but also on the type of natural ecosystem that is replaced. Extensive grazing on many semiarid grasslands, e.g. in Australia and Central Asia, causes relatively small biogeochemical and structural change despite large managed land shares (figures 2(c) and (d), figure S4 in the SI (available at stacks.iop.org/erl/10/044011/mmedia)). On average, Γ values increase with increasing woody vegetation cover, which is why high fractions of land use usually cause lower land use impacts in a grassland or savanna than in a forest landscape. In addition to vegetation structure, grasslands and savannas also differ from forests in regard to their contribution to the global carbon and water cycles, reflected by the global importance component of Γ (figure S3 in the SI available at stacks.iop.org/erl/10/044011/mmedia). Differences in global importance also explain why similar land use fractions usually cause higher impacts in tropical than in temperate

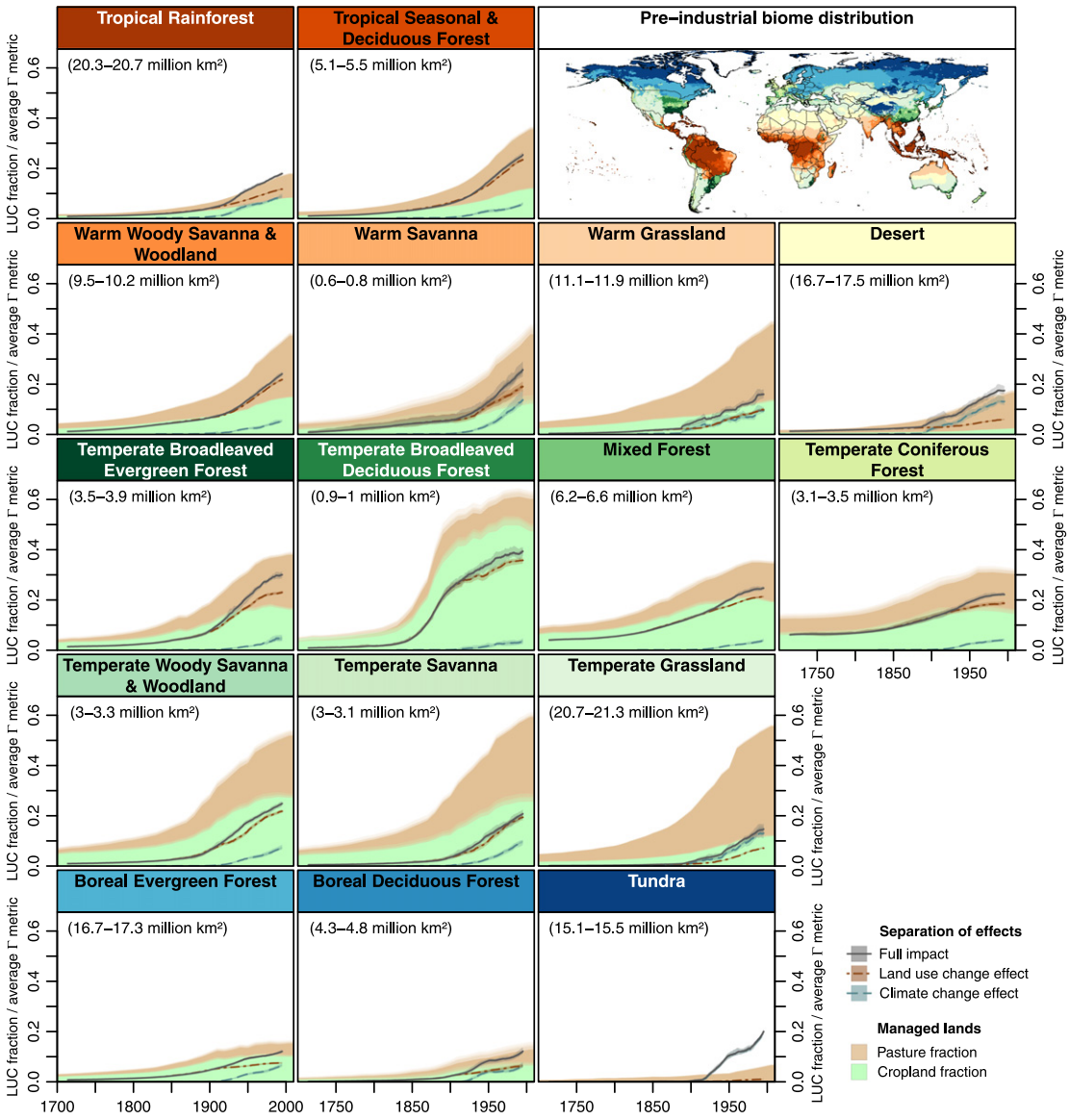

Figure 3. Impact of land use and climate change across biomes. Separate and combined effects at the landscape scale. Map shows potential natural biome distribution under pre-industrial conditions (dominant class from climate ensemble), and numbers in brackets denote ensemble range of biome areas without any land use.

landscapes (figure 3, figure S3 in the SI (available at stacks.iop.org/erl/10/044011/mmedia)).

Table 4 provides lower thresholds of managed land fractions that we have found to cause moderate and major LULCC impacts in each biome today. Numbers represent the 5% quantile of all managed land fractions encountered in grid cells of the biome that result in the respective level of change during the time frame 1981–2010. On the one hand, these numbers serve to illustrate the different extent to which land use impacts various biomes discussed above. On the other hand, they may act as a guideline of the severity of impacts to expect in case of land expansion in landscapes that have little or no land use today. For forest biomes, our results show a risk of moderate LULCC impacts if the managed land fraction exceeds 15–28%, and of major impacts if more than 39–69% of the grid cell is used for agriculture. For savannas and grasslands, the threshold for (moderate) major change is (25–46%) 44–55% managed area. Besides the current land use fraction, climate conditions and land use history also affect the realized LULCC impact in a given landscape. In some regions, such as temperate grasslands, tundra and deserts, climate conditions seem to be a more reliable predictor of land use impacts than the managed land fraction.

3.4. Examples of CC impacts

Changes in vegetation greenness (e.g. Walker *et al* 2012) and advances of the tree line (e.g. Lloyd 2005, MacDonald *et al* 2008) have been observed in both the American and Eurasian tundra. We define any ecosystem with less than 60% tree cover and an annual mean temperature below −2° C as tundra (see figure S5 in the SI (available at stacks.iop.org/erl/10/044011/mmedia)) and find that almost

Table 4. Lower thresholds of managed land fraction leading to moderate ($0.1 < \Gamma < 0.3$) or major ($\Gamma > 0.3$) LULCC impacts in each biome during the time frame 1981-2010.

Impact	$0.1 < \Gamma < 0.3$	$\Gamma > 0.3$
Tropical Rainforest	17%	39%
Tropical Seasonal & Deciduous Forest	20%	42%
Warm Woody Savanna &Woodland	25%	44%
Warm Savanna	30%	48%
Warm Grassland	35%	45%
Temperate Broadleaved Evergreen Forest	24%	47%
Temperate Broadleaved Deciduous Forest	28%	61%
Mixed Forest	19%	44%
Temperate Coniferous Forest	15%	47%
Temperate Woody Savanna & Woodland	31%	55%
Temperate Savanna	39%	47%
Temperate Grassland	46%	46%
Boreal Evergreen Forest	20%	54%
Boreal Deciduous Forest	28%	69%
Tundra	6%	–[a]
Desert	1%	2%

[a] Values are only provided for biomes with at least 1% of their landscapes affected by moderate or major LULCC impacts.

60% of the modelled pre-industrial tundra area is exposed to at least moderate climate-driven changes, with 24% exposed to major shifts, mostly in treeless regions (figure 2(f), figure S6 in the SI (available at stacks.iop.org/erl/10/044011/mmedia)). Along the boreal–tundra ecotone, infilling of sparse tree populations has transformed about one fifth of the tundra into boreal forest (>60% tree cover). Lacking a seed dispersal model, tree establishment in LPJmL is constrained by climatic suitability, not seed availability. Over the course of 100 years, our arctic tree line has shifted by 0–2 grid cells (at 0.5° spatial resolution) and fits well to available maps (figure S7 in the SI (available at stacks.iop.org/erl/10/044011/mmedia)).

Many regions in northern and central Australia have experienced an increase of long-term mean precipitation while the South has generally gotten drier (Jones *et al* 2009). Based on our simulations, wetter conditions combined with the effects of increasing CO_2 concentrations have boosted vegetation productivity over large semiarid and arid areas by a factor of 2 to more than 5, with long-term impacts also on carbon stocks. Plant transpiration has increased with a similar pattern and rate as NPP, whereas changes to evaporation, interception and runoff have been smaller or even showed an opposite sign. Increased fuel load has also increased risk of wildfire in our simulations, especially in more productive grasslands and savannas. Both our model results and observations suggest an expansion of forests into tropical savannas (Brook and Bowman 2006). All of these changes are combined in the Γ metric, leading to major or at least moderate CC effects over much of Australia. Note that many of the affected regions have high fractions of human land use, so other effects such as grazing intensity and prescribed burning practices that are not represented in our model may interfere with the climate signal (Fensham *et al* 2005). These model limitations may also contribute to the very low simulated land use change effect, i.e. why managed lands in much of Australia are biogeochemically very similar to PNV conditions.

We do not explicitly account for impacts of land use change on the climate system. Since our PNV_{CC} and LUC_{CC} simulations use the same observation-based climate data after 1900, we cannot distinguish between LULCC, other anthropogenic and natural forcing on climate. The use of a constant reference climate before 1900 obscures any effect LULCC has had on climate before the onset of modern-day global warming. At the global scale, deforestation has a warming effect through CO_2 emissions, a cooling effect through changes in albedo, and additional effects (both warming and cooling) through reduced emissions of biogenic volatile organic compounds that control other climate pollutants (Unger 2014). Because of additional non-radiative impacts of LULCC, especially through changes to the hydrological cycle, the overall impact of LULCC on global temperatures is unclear, with a likely dominance of the cooling effect in the high latitudes and warming in the tropics and even more complex impacts on precipitation patterns (IPCC 2013).

4. Conclusion

We have quantified human intervention with the terrestrial biosphere through both climate and land use change in a consistent way across the globe and over time. The Γ metric brings together quantitative changes in a high number of system-dynamical parameters, that were previously studied only separately, and allows for the first time to compare the relative strength of these two pressures despite considerable differences in the mechanisms, affected processes and spatial patterns. We have shown that LULCC and CC have now reached a similar level at the global scale, causing average impacts of $\Gamma = 0.11$ and $\Gamma = 0.1$, respectively. In their interaction at the landscape scale, both effects have jointly exposed 55% of the global land surface to at least moderate biogeochemical and vegetation-structural changes of a magnitude comparable to the difference between distinct biomes. CC is the dominant driver of biospheric change on 60% of the land surface. While LULCC is not as widespread as CC, with roughly one third of all landscapes still free of any land use, it has exposed 1.5 times as many landscapes to major impacts as CC.

Land use intensification and industrialization during the 20th century have allowed a rapidly growing world population to shift to a richer diet while per

capita demand for arable land has stabilized or even declined (Ellis *et al* 2013). The future development of land use and its impacts will strongly depend on how much of the anticipated increase in demand for food, feed, fuel and fibre can be met through intensification on existing lands versus expansion of cultivated areas (Foley *et al* 2011, Tilman *et al* 2011, Johnson *et al* 2014). Most land use scenarios project an expansion of cropland which is taken to varying degrees from existing managed grassland or conversion of natural vegetation (van Vuuren *et al* 2011). These choices would result in very different biogeochemical impacts, especially in case of tropical deforestation.

Also, even if the target of limiting global warming to at most 2 K above pre-industrial conditions were met, this would still translate to more than double the warming ecosystems have been exposed to during the 20th century, along with the associated elevated CO_2 concentration and changes in precipitation. In case of continued emissions growth, even 6 K of warming until 2100 seem likely (Rogelj *et al* 2012), putting the majority of ecosystems at risk of major climate-driven transformation (as studied using our Γ metric by Ostberg *et al* 2013, Warszawski *et al* 2013).

The combined impact of possible future changes in land use and climate on landscapes remains to be studied. Our results highlight the importance of considering both drivers in impact assessments, given their comparative magnitude and the potential need for trade-offs in limiting one or the other. For example, land-based climate mitigation measures such as large-scale biomass plantations to substitute fossil fuels, which are often considered crucial to achieving low climate stabilization targets (Rose *et al* 2013), need to be carefully designed to avoid just substituting climate impacts with land use impacts. Overall, the dual pressures of anthropogenic land use expansion and CC have launched a process of global-scale transformation of the Earth's land surface that is accelerating. The mounting shifts in biogeochemical properties of terrestrial landscapes found in our study are likely an indication of developing larger systemic shifts in the Earth system as a whole.

Acknowledgments

This study was supported by GLUES (Global Assessment of Land Use Dynamics, Greenhouse Gas Emissions and Ecosystem Services), a scientific coordination and synthesis project of the German Federal Ministry of Education and Research's (BMBF's) 'Sustainable Land Management' programme (Code01LL0901A).

References

Becker A, Finger P, Meyer-Christoffer A, Rudolf B, Schamm K, Schneider U and Ziese M 2013 A description of the global land-surface precipitation data products of the Global Precipitation Climatology Centre with sample applications including centennial (trend) analysis from 1901–present *Earth Syst. Sci. Data* **5** 71–99

Bondeau A *et al* 2007 Modelling the role of agriculture for the 20th century global terrestrial carbon balance *Glob. Change Biol.* **13** 679–706

Brook B W and Bowman D M J S 2006 Postcards from the past: charting the landscape-scale conversion of tropical Australian savanna to closed forest during the 20th century *Landsc. Ecol.* **21** 1253–66

CRU, University of East Anglia Climatic Research Unit, Jones P D and Harris I (2013). CRU TS3.21: Climatic Research Unit (CRU) Time-Series (TS) Version 3.21 of High Resolution Gridded Data of Month-by-month Variation in Climate (January 1901–December 2012), NCAS British Atmospheric Data Centre

Donohue R J, Roderick M L, McVicar T R and Farquhar G D 2013 Impact of CO2 fertilization on maximum foliage cover across the globe's warm, arid environments *Geophys. Res. Lett.* **40** 3031–35

Ellis E C, Kaplan J O, Fuller D Q, Vavrus S, Klein Goldewijk K and Verburg P H 2013 Used planet: a global history *Proc. Natl Acad. Sci. USA* **110** 7978–85

Ellis E C and Ramankutty N 2008 Putting people in the map: anthropogenic biomes of the world *Front. Ecol. Environ.* **6** 439–47

Esper J and Schweingruber F H 2004 Large-scale treeline changes recorded in Siberia *Geophys. Res. Lett.* **31** L06202

Fader M, Rost S, Müller C, Bondeau A and Gerten D 2010 Virtual water content of temperate cereals and maize: present and potential future patterns *J. Hydrol.* **384** 218–31

Fensham R J, Fairfax R J and Archer S R 2005 Rainfall, land use and woody vegetation cover change in semi-arid Australian savanna *J. Ecol.* **93** 596–606

Foley J A *et al* 2011 Solutions for a cultivated planet *Nature* **478** 337–42

Friedlingstein P, Houghton R A, Marland G, Hackler J, Boden T A, Conway T J, Canadell J G, Raupach M R, Ciais P and Le Quéré C 2010 Update on CO_2 emissions *Nat. Geosci.* **3** 811–2

Gerten D, Rost S, von Bloh W and Lucht W 2008 Causes of change in 20th century global river discharge *Geophys. Res. Lett.* **35** L20405

Gerten D, Schaphoff S, Haberlandt U, Lucht W and Sitch S 2004 Terrestrial vegetation and water balance—hydrological evaluation of a dynamic global vegetation model *J. Hydrol.* **286** 249–70

Haberl H, Erb K H, Krausmann F, Gaube V, Bondeau A, Plutzar C, Gingrich S, Lucht W and Fischer-Kowalski M 2007 Quantifying and mapping the human appropriation of net primary production in earth's terrestrial ecosystems *Proc. Natl Acad. Sci. USA* **104** 12942–7

Harris I, Jones P, Osborn T and Lister D 2014 Updated high-resolution grids of monthly climatic observations—the CRU TS3.10 Dataset *Int. J. Climatol.* **34** 623–42

Heinke J, Ostberg S, Schaphoff S, Frieler K, Müller C, Gerten D, Meinshausen M and Lucht W 2013 A new climate dataset for systematic assessments of climate change impacts as a function of global warming *Geosci. Model Dev.* **6** 1689–703

Heyder U, Schaphoff S, Gerten D and Lucht W 2011 Risk of severe climate change impact on the terrestrial biosphere *Environ. Res. Lett.* **6** 034036

Hoekstra A 1998 *Perspectives on Water: An Integrated Model-Based Exploration of the Future* 1st edn (Utrecht, The Netherlands: International Books)

Hooper D U *et al* 2005 Effects of biodiversity on ecosystem functioning: a consensus of current knowledge *Ecol. Monogr.* **75** 3–35

Houghton R A 2003 Revised estimates of the annual net flux of carbon to the atmosphere from changes in land use and land management 1850–2000 *Tellus* B **55** 378–90

IPCC 2013 *Climate Change 2013: The Physical Science Basis. Working Group I Contribution to the Fifth Assessment Report of the Intergovernmental Panel on Climate Change* (Cambridge, UK: Cambridge University Press)

IPCC 2014a *Climate Change 2014: Impacts, Adaptation, and Vulnerability: A. Global and Sectoral Aspects. Contribution of Working Group II to the Fifth Assessment Report of the Intergovernmental Panel on Climate Change* (Cambridge, UK: Cambridge University Press)

IPCC 2014b *Climate Change 2014: Impacts, Adapation, and Vulnerability: B. Regional Aspects. Contribution of Working Group II to the Fifth Assessment Report of the Intergovernmental Panel on Climate Change* (Cambridge, UK: Cambridge University Press)

Johnson J A, Runge C F, Senauer B, Foley J and Polasky S 2014 Global agriculture and carbon trade-offs *Proc. Natl Acad. Sci. USA* **111** 12342–7

Jones D A, Wang W and Fawcett R 2009 High-quality spatial climate data-sets for Australia *Aust. Meteorol. Oceanogr. J.* **58** 233–48

Kaplan J O, Krumhardt K M, Ellis E C, Ruddiman W F, Lemmen C and Goldewijk K K 2011 Holocene carbon emissions as a result of anthropogenic land cover change *Holocene* **21** 775–91

Keeling C D, Piper S C, Bacastow R B, Wahlen M, Whorf T P, Heimann M and Meijer H A 2001 Exchanges of Atmospheric CO_2 and $13CO_2$ with the Terrestrial Biosphere and Oceans from 1978 to 2000: I. Global Aspects, SIO Reference, Scripps Institution of Oceanography *San Diego* (San Diego: Scripps Institution of Oceanography) (http://escholarship.org/uc/item/09v319r9)

Kirch P V 2005 Archaeology and global change: The Holocene record *Annu. Rev. Environ. Resour.* **30** 409–40

Klein Goldewijk K, Beusen A, van Drecht G and de Vos M 2011 The HYDE 3.1 spatially explicit database of human-induced global land-use change over the past 12000 years *Glob. Ecol. Biogeogr.* **20** 73–86

Klein Goldewijk K and van Drecht G 2006 HYDE 3. Current and historical population and land cover *Integrated Modelling of Global Environmental Change. An Overview of IMAGE 2.4* ed A F Bouwman *et al* (Bilthoven, The Netherlands: Netherlands Environmental Assessment Agency (MNP))

Klein Goldewijk K and Verburg P H 2013 Uncertainties in global-scale reconstructions of historical land use: an illustration using the HYDE data set *Landsc. Ecol.* **28** 861–77

Krausmann F, Erb K-H, Gingrich S, Haberl H, Bondeau A, Gaube V, Lauk C, Plutzar C and Searchinger T D 2013 Global human appropriation of net primary production doubled in the 20th century *Proc. Natl Acad. Sci. USA* **110** 10324–9

Lloyd A H 2005 Ecological histories from Alaskan tree lines provide insight into future change *Ecology* **86** 1687–95

MacDonald G M, Kremenetski K V and Beilman D W 2008 Climate change and the northern Russian treeline zone *Philos. Trans. R. Soc.* B **363** 2285–99

Mooney H, Larigauderie A, Cesario M, Elmquist T, Hoegh-Guldberg O, Lavorel S, Mace G M, Palmer M, Scholes R and Yahara T 2009 Biodiversity, climate change, and ecosystem services *Curr. Opin. Environ. Sustain.* **1** 46–54

New M, Hulme M and Jones P 2000 Representing twentieth-century space-time climate variability: II. Development of 1901–96 monthly grids of terrestrial surface climate *J. Clim.* **13** 2217–38

Ostberg S, Lucht W, Schaphoff S and Gerten D 2013 Critical impacts of global warming on land ecosystems *Earth Syst. Dyn.* **4** 347–57

Parmesan C 2006 Ecological and evolutionary responses to recent climate change *Annu. Rev. Ecol. Evol. Syst.* **37** 637–69

Parmesan C 2007 Influences of species, latitudes and methodologies on estimates of phenological response to global warming *Glob. Change Biol.* **13** 1860–72

Parmesan C and Yohe G 2003 A globally coherent fingerprint of climate change impacts across natural systems *Nature* **421** 37–42

Pongratz J, Reick C, Raddatz T and Claussen M 2008 A reconstruction of global agricultural areas and land cover for the last millennium *Glob. Biogeochem. Cycles* **22** GB3018

Portmann F T, Siebert S and Döll P 2010 MIRCA2000-Global monthly irrigated and rainfed crop areas around the year 2000: a new high-resolution data set for agricultural and hydrological modeling *Glob. Biogeochem. Cycles.* **24** GB1011

Rogelj J, Meinshausen M and Knutti R 2012 Global warming under old and new scenarios using IPCC climate sensitivity range estimates *Nat. Clim. Change* **2** 248–53

Rohwer J, Gerten D and Lucht W 2007 Development of functional irrigation types for improved global crop modelling *Technical Report 104* (Potsdam, Germany: Potsdam Institute for Climate Impact Research)

Rose S K, Kriegler E, Bibas R, Calvin K, Popp A, van Vuuren D P and Weyant J 2013 Bioenergy in energy transformation and climate management *Clim. Change* **123** 477–93

Rost S, Gerten D and Heyder U 2008 Human alterations of the terrestrial water cycle through land management *Adv. Geosci.* **18** 43–50

Schaphoff S, Heyder U, Ostberg S, Gerten D, Heinke J and Lucht W 2013 Contribution of permafrost soils to the global carbon budget *Environ. Res. Lett.* **8** 014026

Schneider U, Becker A, Finger P, Meyer-Christoffer A, Rudolf B and Ziese M 2011 *GPCC full data reanalysis version 6.0 at 0.5°: monthly land-surface precipitation from rain-gauges built on GTS-based and historic data* Global Precipitation Climatology Centre (GPCC, http://gpcc.dwd.de/) at Deutscher Wetterdienst

Sitch S *et al* 2003 Evaluation of ecosystem dynamics, plant geography and terrestrial carbon cycling in the LPJ dynamic global vegetation model *Glob. Change Biol.* **9** 161–85

Sitch S *et al* 2008 Evaluation of the terrestrial carbon cycle, future plant geography and climate-carbon cycle feedbacks using five Dynamic Global Vegetation Models (DGVMs) *Glob. Change Biol.* **14** 2015–39

Steffen W, Crutzen P J and McNeill J R 2007 The Anthropocene: are humans now overwhelming the great forces of nature *Ambio* **36** 614–21

Stone D *et al* 2013 The challenge to detect and attribute effects of climate change on human and natural systems *Clim. Change* **121** 381–95

Sykes M T, Prentice I C and Laarif F 1999 Quantifying the impact of global climate change on potential natural vegetation *Clim. Change* **41** 37–52

Thonicke K, Venevsky S, Sitch S and Cramer W 2001 The role of fire disturbance for global vegetation dynamics: coupling fire into a Dynamic Global Vegetation Model *Glob. Ecol. Biogeogr.* **10** 661–77

Tilman D, Balzer C, Hill J and Befort B L 2011 Global food demand and the sustainable intensification of agriculture *Proc. Natl Acad. Sci. USA* **108** 20260–4

Unger N 2014 Human land-use-driven reduction of forest volatiles cools global climate *Nat. Clim. Change* **4** 907–10

Van Vuuren D P *et al* 2011 The representative concentration pathways: an overview *Clim. Change* **109** 5–31

Waha K, van Bussel L G J, Müller C and Bondeau A 2012 Climate-driven simulation of global crop sowing dates *Glob. Ecol. Biogeogr.* **21** 247–59

Walker D A *et al* 2012 Environment, vegetation and greenness (NDVI) along the North America and Eurasia Arctic transects *Environ. Res. Lett.* **7** 015504

Warszawski L *et al* 2013 A multi-model analysis of risk of ecosystem shifts under climate change *Environ. Res. Lett.* **8** 044018